Evaluating the Thermal Performance of Active Envelopes

Dirk Saelens

Hugo Hens, Ph.D.
Member ASHRAE

ABSTRACT

Active envelopes are presented as energy-efficient envelope solutions. In this paper, a numerical model to evaluate the thermal behavior of active envelopes is discussed and compared with in situ measurements. The agreement between the measurements and the simulations is good for the mechanical flow active envelope, but less so for the natural flow variant. After implementing the numerical model in an energy simulation program, an annual energy simulation on a selected number of active envelope typologies has been performed and compared to a classical cladding system. The U-factor and g-value of active envelope systems become dependent on the system properties and even on the climatic conditions for natural flow envelopes. To correctly evaluate the energy efficiency of active envelopes, it is imperative to take into account the enthalpy change of the cavity air.

INTRODUCTION

Nowadays, the sensibility for environmentally friendly and energy-conscious building design is an important issue among building designers. As envelopes form the boundary between the exterior environment and the interior, they have a considerable effect on the energy efficiency of the building. However, energy efficiency is not the only concern. Some particular envelopes are designed to keep up with architectural styles or to evoke a high-tech image. Furthermore, envelopes form an acoustical shelter, give the possibility to naturally ventilate a building, provide daylight, and should, in general, comply with an array of performances (Hendriks and Hens 2000).

The development of active envelopes fits into the described context above. Active envelopes (also known as double-skin facades, twin facades, or second-skin facades) consist of two panes with a cavity in between through which air flows. In the cavity, a shading device is usually provided. Generally, distinction is made between naturally and mechanically ventilated active envelopes. Regarding the path the air follows, several ventilation strategies are possible. Extensive literature on active envelope typologies can be found in Compagno (1995), Gertis (1999), Ziller (1999), and Baker et al. (2000).

Active envelopes originate from the Scandinavian countries (Park et al. 1989) and have become very popular in the European countries. Some eye-catching projects from renowned architects, such as the Briarcliff House in Farnborough (1984, United Kingdom), the Commerzbank Tower in Frankfurt am Main (1993, Germany), and the Debis building in Berlin (1996, Germany), are regularly discussed in literature. In the United States, however, active envelopes are less common. Only a few examples can be found, for instance, the Hooker Office Building in Niagara Falls (1980).

Regarding energy efficiency, two operational modes are mentioned: (1) active envelopes used as air-air heat exchangers and (2) active envelopes as solar collectors. The first mode aims at diminishing and recovering transmission losses through the inner pane. Although interesting as an idea for dwellings, the objective of gathering energy in office buildings with high internal gains is debatable. The second mode has two aims— during the heating season, solar energy may be used to preheat the air supplied to the HVAC system. During summer, the collected solar energy from the cavity is expelled

Dirk Saelens is a Ph.D. student and **Hugo Hens** is a professor in the Department of Civil Engineering, Laboratory of Building Physics, Katholieke Universiteit Leuven, Leuven, Belgium.

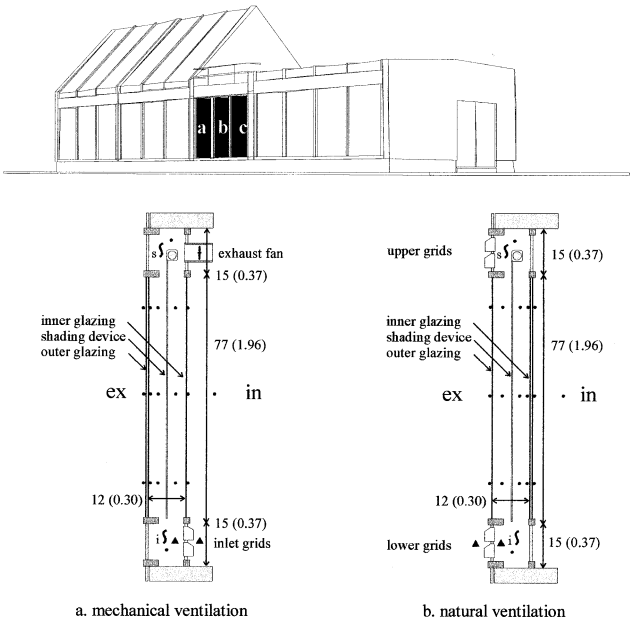

Figure 1 *The Vliet test building. The position of the experimental setup at the southwest facade: (a) classical cladding system, (b) mechanically ventilated facade, and (c) naturally ventilated facade. Cross section through the mechanically (a) and naturally (b) ventilated active envelope system showing the position of the measuring points. Points (•) represent thermocouples, pairs of triangles (◢◢) represent pressure difference measurements, and curves show tracer gas inlet* $\left(\int_i\right)$ *and sampling* $\left(\int_s\right)$ *point. Main dimensions are given in inches (m).*

to reduce the cooling load. This implies that the shortwave solar energy has to be absorbed to be carried away by the airflow. To be efficient, high cavity temperatures are necessary, inevitably increasing the indirect gains. These two modes are applicable on both the mechanically and naturally ventilated variants. Furthermore, natural flow active envelopes may be developed to allow natural ventilation in high-rise buildings. A detailed experimental investigation of room ventilation with natural flow active envelopes can be found in Ziller (1999).

In the present paper, a numerical model to evaluate the thermal performance of active envelopes is proposed and is compared to in situ measurements at the Vliet test building of the Laboratory of Building Physics (Figure 1). The numerical model is implemented in a building energy simulation program and is used to run an annual energy simulation of an office equipped with two variants of active envelopes. This gives the ability to find out whether the above described operational modes work and the ability to compare the two variants

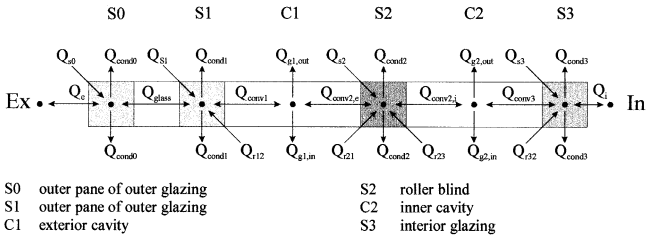

Figure 2 *Diagram of the numerical model for an active envelope with forced convection and lowered shading device.*

with each other and with a traditional cladding system. From this model, standard performance indicators, such as the U-factor and the g-value, are derived and discussed.

NUMERICAL MODEL

Model Description

The numerical model is based on a cell-centred finite-volume method (CVM). The active envelope is vertically divided into four or five layers (depending on whether the roller blind is raised or lowered), which are divided into 32 parts along the height. For each volume, the heat balance is written and solved simultaneously (Figure 2). At the cavity surfaces (S1, S2, and S3), three heat transfer mechanisms occur—conduction (Q_{cond}), convection (Q_{conv}), and radiation (Q_r). The convective heat transfer (Q_{conv}) depends on the airflow rate and temperature difference between the surface and the air. Radiant heat transfer (Q_r) for each surface is calculated with the net-radiation method (Hottel 1954; Siegel and Howell 1992). In the cavities (C1 and C2), the heat transfer is governed by convection and enthalpy transport due to the airflow. Heat transfer between the two panes of the double glazing (Q_{glass}) is a combination of conduction, convection, and radiation and is calculated from manufacturers' data. The absorbed solar energy (Q_s) is calculated for each separate layer with an embedded technique described by Edwards (1977). This method allows the ability to take into account all internal reflections. The absorbed solar energy is a function of the angle of incidence and takes into account partial shading of the panes. The heat transfer with the surroundings (Q_e and Q_i) is described with a combined heat transfer coefficient. Long-wave radiation at the outside is taken into account by means of an equivalent outdoor temperature. It is assumed that the air from the outer cavity cannot flow through the roller blind toward the inner cavity or vice versa. This assumption has been verified with tracer gas measurements and proved to be valid for the specific conditions of the active envelopes considered in this study.

With the above-described model, both mechanically and naturally ventilated active envelopes can be modeled. The airflow rate in the mechanical flow variant is a known variable and, hence, the solution of the thermal system is obvious. The

airflow rate and the temperature profiles in the naturally ventilated active envelope are mutually dependent and, hence, the thermal system is to be solved iteratively. The pressure difference (Δp), due to thermal buoyancy, has been determined with the following expression (Liddament 1996):

$$\Delta\rho = \rho_0 \cdot g \cdot H \cdot \left(\frac{T_{cav}}{T_e} - 1\right) \quad (1)$$

with ρ_0 the air density, g the gravitational acceleration, H the cavity height, T_{cav} the absolute average cavity temperature, and T_e the absolute outdoor temperature. This pressure difference is balanced by the airflow resistance of the cavity.

A parameter analysis (Saelens and Hens 2001b) shows that the simulations are particularly sensitive to the distribution of the airflow rate in both cavities, the overall airflow rate, the heat transfer coefficient in the cavities, the absorbed solar energy (dependent on the angle of incidence), and the inlet temperature.

Comparison with Measured Data

In an effort to evaluate the energetic performance of active envelopes, an experimental setup for active envelopes was constructed at the Vliet building of the Laboratory of Building Physics in Leuven, Belgium. The following three facade systems were installed: (1) a classical cladding system with external shading device, (2) a mechanical flow active envelope, and (3) a naturally ventilated active envelope (Figure 1). The envelopes face southwest. The cells in which the envelope systems were built measure 1.2 m (47 in.) wide by 2.7 m (106 in.) high by 0.5 m (20 in.) deep. The variant with mechanical flow (Figure 1a) is ventilated with interior air by means of a speed controllable circular duct fan that can provide an airflow between 30 and 150 m³/h (229 and 1144 cfm). The air flows up from the bottom. The double glazing is positioned at the outside. As the natural flow variant (Figure 1b) is ventilated with exterior air, the double glazing for the naturally ventilated variant is situated at the inside. The direction of the airflow strongly depends on the wind speed and wind direction (Saelens and Hens 2001a). The double glazing in both cases is an argon-filled double-glazed unit (4-15-4 mm [0.16-0.59-0.16 in.]) with low-E coating (coating emissivity = 0.09). According to the manufacturers' data, the U-factor of this glazing is 1.23 W/(m²·K) (0.217 Btu/[h·ft²·°F]) and the g-value is 0.64. The other pane consists of single clear glass (8 mm [0.31 in.]). Both systems are provided with an automated roller blind in the middle of the cavity.

Surface temperatures were measured at both sides of the double-pane glazing and at one side of the single-pane glazing. The cavity air temperature was monitored on either side of the shading device. This cross-sectional setup was installed at three different heights in order to measure temperature gradients along the height. The air inlet and outlet temperatures, as well as the interior temperature in front of each system, were monitored. The air pressure difference was measured with pressure tubes connected to a differential pressure transducer. With a calibrated fan, a relation between the pressure difference over the inlet grid and the airflow rate was found.

$$\begin{aligned} G_a &= 64 \cdot \Delta p^{0.44} [(\mathrm{m}^3/\mathrm{h}),\ \Delta p \text{ in Pa}]; \\ G_a &= 23300 \cdot \Delta p^{0.44} [\mathrm{cfm},\ \Delta p \text{ in psi}] \end{aligned} \quad (2)$$

This relation was used to deduce the airflow rate from the pressure difference over the inlet grid and to determine the airflow resistance of the cavity.

Figures 1a and 1b show the position of the thermocouples (represented as dots), the tracer gas inlet and sampling points (represented as curves), and the pressure difference measurement tubes (represented as triangles). Data were measured every 3 minutes and averaged on a 15-minute basis. Meteorological data were gathered by an automatic weather station from which 15-minute averages are used. The station measures the wind speed and wind direction, the total horizontal solar radiation, the vertical incident solar radiation on the southwest orientated surface, the air temperature, and the relative humidity.

When the shading device is lowered, the cavity is divided into two parts. The distribution of the airflow over the two cavities has been experimentally determined with tracer gas measurements. It was shown that for the mechanically ventilated envelope, approximately 25% of the airflow rate flew through the exterior cavity and 75% flew through the interior cavity. The distribution of the airflow in the natural flow variant is much more complex and depends on wind speed and wind direction.

As an example, the measured temperature profiles of February 16, 2000, are compared with simulations for both the mechanical (Figure 3) and natural (Figure 4) flow variant. For the mechanically ventilated active envelope, the overall agreement between the measurements and the simulations is very good (Figure 3). Figure 3b clearly shows the effect of the airflow distribution. Because of the lower airflow rate in the outer cavity, the curvature of the temperature profile of the outer cavity (T_{ae}) is bigger than that of the inner cavity (T_{ai}). The agreement between the measurements and simulations for the naturally ventilated active envelope is not as good (Figure 4). This is mainly due to the fact that the airflow rate and airflow distribution over the cavities cannot be predicted accurately. In general, the simulations deviate more from the measured data for higher wind speeds. In both cases, the simulations underestimate the measured temperatures on the outer pane during daytime. Busselen and Mattelaer (2000) show that this is due to the heating of the thermocouples by solar radiation.

ENERGY PERFORMANCE ASSESSMENT

Description of Envelope Variants and Office

Active envelopes are regularly praised for having superior energy performance over traditional cladding solutions. In

this section, an annual energy simulation on an hourly basis under Belgian climatic conditions has been performed for a one-person office facing south. A traditional European cladding solution (traditional) will be compared to a naturally (natural) and a mechanically (FOR *x*, where *x* represents the office air change rate) ventilated active envelope system in order to find whether active envelopes actually outperform traditional solutions. Envelope details can be found in Figure 5. The mechanically ventilated active envelopes are ventilated with three different airflow rates: (1) the ventilation airflow rate as a minimum: $G_a = G_v$ = 30 m³/h (229 cfm) or 0.5 ACH (FOR 0.5), (2) double ventilation rate: G_a = 60 m³/h (458 cfm) corresponding to an air change rate of 1.0 (FOR 1.0), and (3) G_a = 120 m³/h (915 cfm) or 2.0 ACH (FOR 2.0). The airflow rate through the mechanically ventilated active envelope is kept constant throughout the entire calculation.

The office measures 4 by 6 by 2.5 m (13 by 20 by 8 ft) (width by depth by height). The glass-to-wall ratio is approximately 60%, the transparent surface measures 3.00 by 2.25 m (118 by 89 in.), and the opaque part of the wall consists of an insulated cladding system with a U-factor of 0.33 W/(m²·K) (0.058 Btu/[h·ft²·°F]). The setpoint temperature for heating is 21°C (70°F), with a night setback to 16°C (61°F); the setpoint temperature for cooling is 26°C (79°F). Internal gains due to occupancy, lighting, and office appliances have been taken into account according to the ASHRAE guidelines (ASHRAE 1997). All systems are equipped with a roller blind shading device, which is lowered as soon as the direct solar radiation, impinging on the surface, exceeds 150 W/m² (48 Btu/[h·ft²]). The present results have to be seen as best practice. A recent study (Saelens and Hens 1999) of a real life building equipped with mechanically ventilated active envelopes indicated that air infiltration in the cavity and poorly insulated return ducts strongly affect the performance of the mechanical flow variant.

Energy Demand Analysis

Transmission. Many authors suggest that active envelopes are useful to lower transmission losses and gains through transparent parts of the envelope. Figure 6 shows the trans-

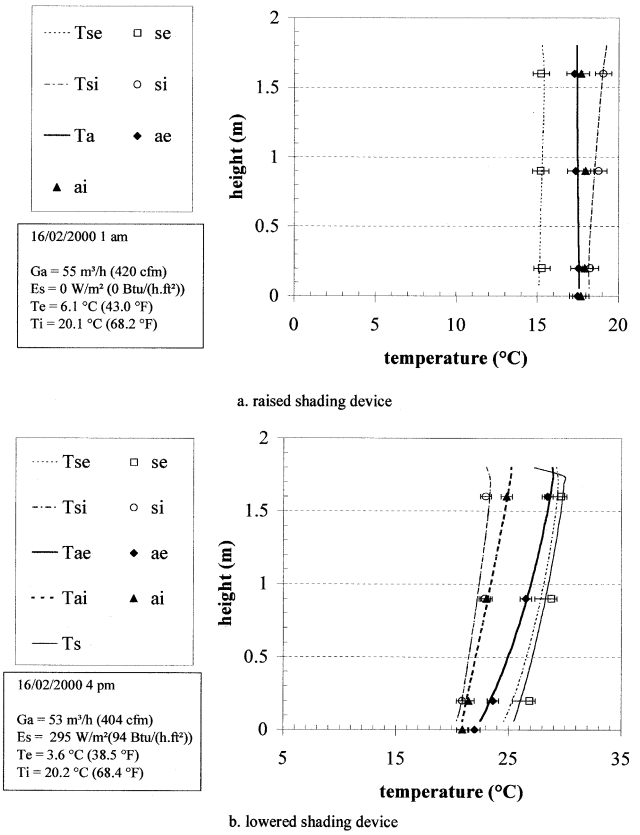

Figure 3 *Comparison of the measured and simulated temperature profiles for the mechanical flow variant with (a) raised and (b) lowered shading device. (Subscripts:* se*: exterior surface [S1],* ae*: exterior cavity [C1],* s*: shading device [S2],* ai*: interior cavity [C2],* si*: interior surface [S3].)*

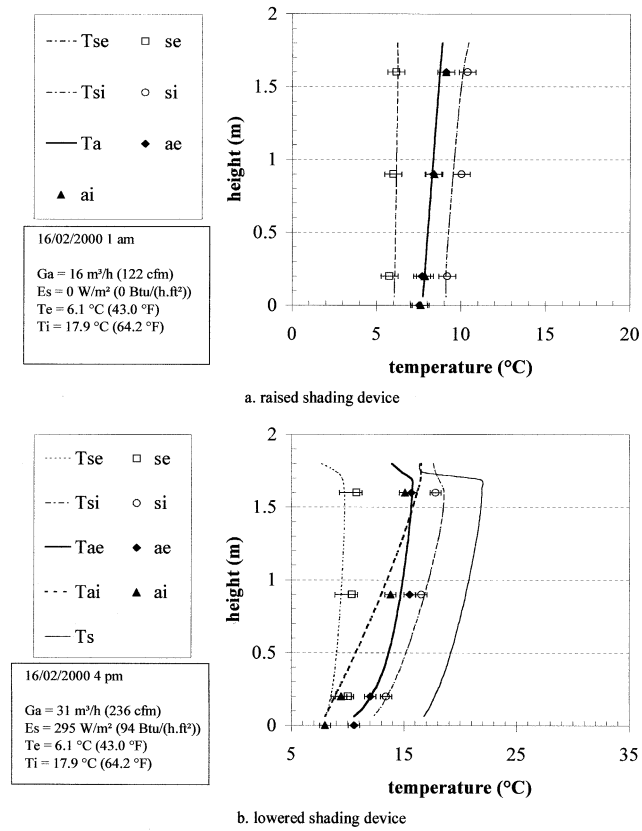

Figure 4 *Comparison of the measured and simulated temperature profiles for the natural flow variant with (a) raised and (b) lowered shading device. (Subscripts:* se*: exterior surface [S1],* ae*: exterior cavity [C1],* s*: shading device [S2],* ai*: interior cavity [C2],* si*: interior surface [S3].)*

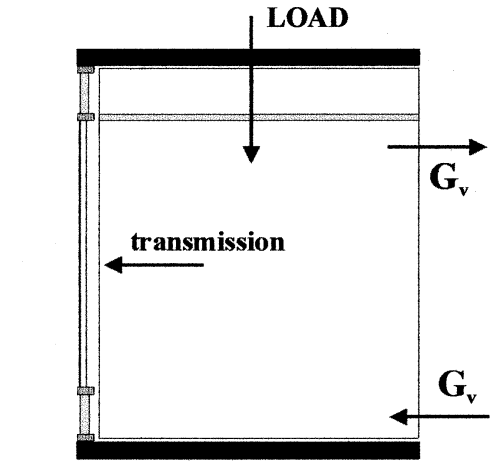

a. Traditional solution (traditional)

Traditional cladding system with highly insulated glazing (U-factor = 1.23 W/ [m^2·K] [0.217 Btu/(h·ft^2·°F)], g-value = 0.59) and exterior shading device (g-value combined system [glass and shading device] = 0.15).

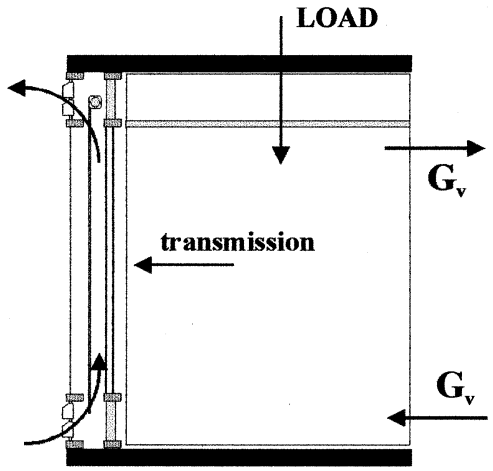

b. Natural ventilation (natural)

Naturally-ventilated cavity, the air flows from the exterior to the exterior. The grids are not adjustable. The active envelope is not used to ventilate the office.

Outer pane: single glazing, U-factor = 5.67 W/(m^2·K) (0.999 Btu/[h·ft^2·°F]); inner pane: double glazing, U-factor = 1.23 W/(m^2·K) (0.217 Btu/[h·ft^2·°F]).

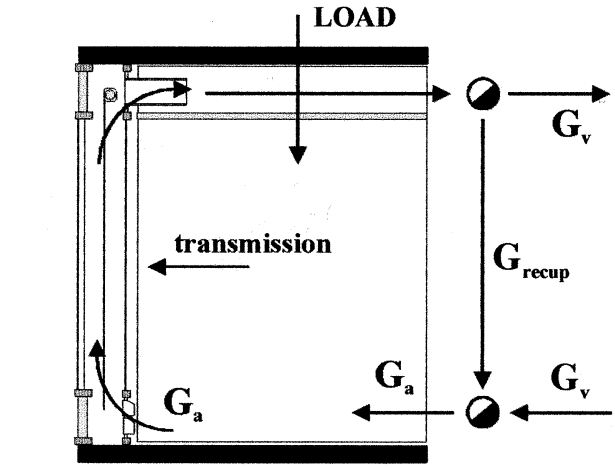

c. Mechanical ventilation (FOR 0.5, FOR 1.0, and FOR 2.0)

Mechanically-ventilated cavity, the air flows from the interior to the HVAC-plant where it is either reused or expelled. Three different airflow rates (G_a) are investigated: 30, 60, and 120 m^3/h (229, 458, and 915 cfm) corresponding to air change rates of 0.5, 1.0, and 2.0 ACH.

Outer pane: double glazing, U-factor = 1.23 W/(m^2·K) (0.217 Btu/[h·ft^2·°F]); inner pane: single glazing, U-factor = 5.67 W/(m^2·K) (0.999 Btu/[h·ft^2·°F]).

Figure 5 *Overview of the analyzed office variants.*

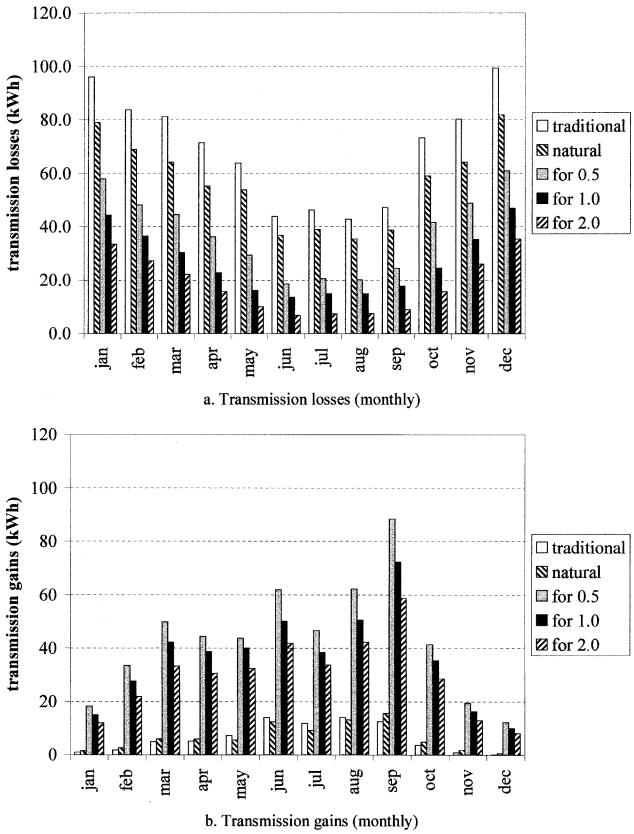

Figure 6 *Monthly transmission losses (a) and gains (b) through the transparent surface of the office for different envelope typologies.*

mission losses and gains through the transparent part of the active envelope (indicated with transmission on Figure 5) for the different cases.

Figure 6a indicates that both the naturally and mechanically ventilated active envelopes have lower transmission losses than the traditional solution. On an annual basis, the naturally ventilated variant decreases the transmission losses by approximately 18% compared to the traditional solution. By adding an extra pane, the overall thermal transmittance lowers and the solar energy can be captured more efficiently. The mechanically ventilated variants perform even better. Depending on the airflow rate, the annual transmission losses decrease with 46% (FOR 0.5), 62% (FOR 1.0), and 74% (FOR 2.0) compared to the traditional solution. As the air comes from the inside, the mechanical flow variant has lower transmission losses if the airflow rate is increased. Furthermore, the solar energy can again be captured more efficiently.

Figure 6b shows that the transmission gains of the traditional and naturally ventilated envelope are of the same magnitude. The transmission gains of the mechanically ventilated active envelopes are four to seven times higher. In the summer, the cooling effect of the outside air in the naturally ventilated variant proves to be beneficial as it lowers the indirect solar gains. The mechanical flow variant represents the highest indirect solar gains—the captured solar energy raises the cavity temperature considerably and, due to the low thermal resistance of the inner pane, the indirect gains raise substantially. Increasing the airflow rate of the mechanical flow active envelopes reduces the cavity temperature and, hence, the indirect gains. Furthermore, the high surface temperatures, which are beneficial during winter, affect the thermal comfort near the envelope in the summer and may cause radiation asymmetry. The surface temperature easily exceeds 35°C (95°F), values that are confirmed by measurements on a real-life building (Saelens and Hens 1998).

Office Load. From the analysis of the transmission losses (Figure 6a), one could conclude that active envelopes, and especially mechanically ventilated envelopes with high airflow rates, lower the heating demand. Regarding transmission gains (Figure 6b), the traditional and naturally ventilated active envelope have considerably lower gains than the mechanically ventilated variant. The gains of the latter can be lowered by ventilating the cavity. However, the transmission losses do not necessarily reflect the actual heating or cooling load of the office (indicated with load on Figure 5). The load of the office is defined as the amount of energy needed to keep the office temperature between the previously defined setpoint temperatures. The way the load is inserted in the office is not considered in the energy demand analysis.

In all cases, the minimum supply of fresh air is set to 30 m³/h (229 cfm) or 0.5 ACH (G_v on Figure 5). However, mass conservation demands that the supply of air increases if the airflow rate in the mechanically ventilated active envelope exceeds the ventilation airflow rate. Hence, the total airflow rate G_a is higher then the ventilation rate for the cases FOR 1.0 and FOR 2.0. As indicated in Figure 5c, the airflow rate above the ventilation rate may be recovered ($G_{recup} = G_a - G_v$ on Figure 5c) whenever appropriate (for instance, full recovery in winter and no recovery in summer).

Figure 7 shows that we have to pay a price for the reduction of the transmission losses—a reduction of the enthalpy content compared to the interior air. The cavity air enthalpy change (ΔE) is calculated as

$$\Delta E = \rho_a \cdot c_a \cdot G_a \cdot (T_{in} - T_{outlet}) . \qquad (3)$$

Figure 7 indicates that the idea of recovering the transmission losses and using the active envelope as a solar collector to reduce the heating demand does not work. Analysis of the return air temperature in the heating season (Figure 7a) shows that the enthalpy losses are much higher than the gains. The maximum gains (negative values) can be found in the summer (Figure 7b) when we need them less. The resulting heating load (Figure 8a) and cooling load (Figure 8b) show quite a different picture from the transmission losses and gains (Figure 6).

Figure 8a shows the resulting heating load. If we take the traditional envelope as a reference, we notice that in spite of the largest transmission losses, the traditional envelope has the

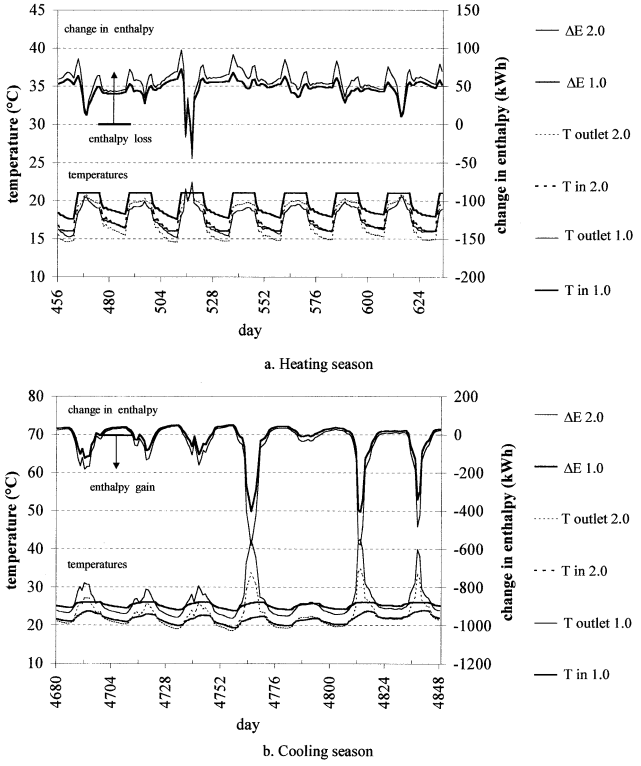

Figure 7 *Enthalpy loss and gain for the mechanically ventilated active envelope with airflow rates above the ventilation rate.*

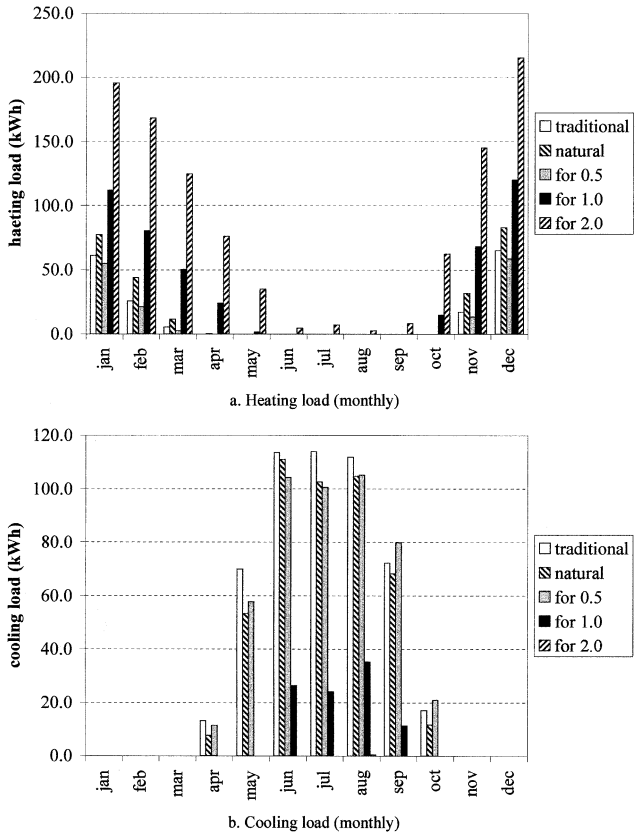

Figure 8 *Monthly office heating (a) and cooling (b) load.*

second lowest heating load. Only the active envelope, which is ventilated with the ventilation rate (0.5 ACH) (FOR 0.5), performs better. This again stresses that we have to pay a price to lower the transmission losses by increasing the airflow rate.

Comparing the variants where only the ventilation airflow rate is used (traditional, natural, and FOR 0.5) to ventilate the office, we see that the naturally ventilated variant has higher heating loads and that the mechanically ventilated variant has slightly lower heating loads. The increase in heating load can be explained by the lower direct solar gains—because of the extra pane, the overall solar transmittance of the naturally ventilated variant is lower. The lower heating load for the mechanically ventilated variant reflects the lower transmission losses. In this case, the enthalpy losses do not matter as only the ventilation airflow, which is not reused, flows through the envelope. Because of the lower direct solar gains for the mechanically ventilated windows, the decrease in heating load is less pronounced than might be expected from the decrease in transmission losses (Figure 6a). The moment the airflow rate increases (cases FOR 1.0 and FOR 2.0), we notice that the decrease in transmission losses is offset by the increase in enthalpy losses—the heating load increases with increasing airflow rate and largely exceeds the heating load of the traditional envelope.

Figure 6b indicates that the mechanically ventilated active envelopes have the highest transmission gains. We would expect to find the highest cooling loads for these variants. Figure 8b, however, indicates that this is not the case. The cooling load of the variants, where only the ventilation airflow rate is used (traditional, natural, and FOR 0.5), have comparable cooling loads. The cooling loads for the traditional envelope are slightly higher because of the higher solar transmittance. Active envelope systems with higher ventilation rates (FOR 1.0 and FOR 2.0) clearly reduce the cooling load. However, this is not a consequence of the reduction in transmission gains by the active envelope but is caused by the increased ventilation rate. It should be noted that the use of fan power is not included in this analysis.

The Use of Standard Energy Performance Indicators. From the previous sections, it is clear that traditional energy performance indicators such as the U-factor and the g-value are only to be seen as envelope level performance indicators, useful to determine, for instance, local thermal comfort or to illustrate the behavior of active envelopes. Under normal conditions, the U-factor and the g-value only depend on the material properties and thickness of the envelope layers. The U-factor of an active envelope, however, also depends on the system's properties—the airflow rate, the position of the shading device, the typology, etc. In this section, the U-factor and g-value will be used to illustrate the importance of the inlet

temperature, the influence of the airflow rate, and the influence of the solar incidence angle.

The U-factor normally determines the rate of heat transfer in the absence of sunlight, air infiltration, and moisture condensation (ASHRAE 1997). Due to the airflow through the cavity, the heat flux perpendicular to the envelope becomes a function of the height. Taking the heat flux through the inner pane as a reference, the U-factor of active envelope systems may be defined as

$$U = \frac{1}{H} \cdot \frac{1}{R} \cdot \frac{1}{\theta_i - \theta_e} \cdot \int_0^H (\theta_j(z) - \theta_i) \cdot dz \qquad (4)$$

where R represents the inner pane thermal resistance with inclusion of the internal surface film resistance, H is the pane height, $\theta_j(z)$ is the inner pane temperature as a function of height, and $\theta_i - \theta_e$ is the temperature difference between the inside and the outside. U-factors are a powerful means to describe the heat transfer through envelope parts. However, in the case of active envelopes, due to the airflow through the cavity, the shading device, and the many possible typologies, the U-factor becomes a hard-to-use, typology-dependent, multidimensional function of system and material properties.

As an example, Figure 9 gives the U-factor for the mechanical flow variant as a function of inlet temperature and airflow rate. Considering the ideal case in which the inlet temperature equals the interior temperature (20°C [68°F]), we calculate a U-factor between 0.18 (0.032) and 0.60 W/(m²·K) (0.11 Btu/[h·ft²·°F]) for an airflow rate between 10 m³/(h·m) (23 cfm/in.) and 200 m³/(h·m) (465 cfm/in.). The transmission losses through the interior pane decrease with increasing airflow rate. We notice that the inlet temperature strongly influences the U-factor—the transmission losses change linearly with the inlet temperature. For inlet temperatures above 21°C (70°F), even negative U-factors are calculated. An air intake temperature drop of 1 K (1°F), for instance, due to badly insulated frames or air infiltration, increases the U-factor with 0.18 W/(m²·K²) (0.018 Btu/[h·ft²·°F]) for an airflow rate of 100 m³/h (763 cfm). This awareness stresses the importance of good workmanship and design.

The g-value, or solar transmittance, is defined as the ratio of the total energy flux ($q_{dir} + q_{ind}$) into the building to the total solar radiation. When calculating the g-value, the interior and exterior temperatures are set to zero to account for solar radiation only. The g-value for active envelopes may be defined as

$$g = \frac{q_{dir} + q_{ind}}{E_S} = \frac{\tau_k \cdot E_S + \frac{1}{H} \cdot \frac{1}{R} \cdot \int_0^H \theta_j(z) \cdot dz}{E_S} \qquad (5)$$

where τ_k is the shortwave solar transmittance of the whole system, E_S is the total incoming solar radiation impinging on the surface, H is the pane height, R represents the inner pane thermal resistance with inclusion of the internal surface film resistance, and $\theta_j(z)$ is the inner pane temperature as a function of height.

Again, the solar transmittance will be influenced both by material and system properties. Figure 10 illustrates the variation of the dynamic g-value with the angle of incidence and the airflow rate for the mechanical flow variant. The g-value is relatively constant for an incidence angle from 0 to 50 degrees. For higher angles of incidence, reflectivity becomes more pronounced, which results in a decrease of the g-value. As the airflow rate increases, the amount of air cooling down the cavity increases, the indirect gains decrease, and, hence, the g-value lowers.

Regarding naturally ventilated cavities, one could perform the same analysis. Again the U-factor and g-value are dependent on the system properties. However, for the naturally ventilated cavity, the airflow and, hence, the results, depend on the climatic conditions—solar irradiation, temperature difference between the cavity and the outside, wind speed, and wind direction. Because of this dependency, the meaning of the U-factor and the g-value becomes even more

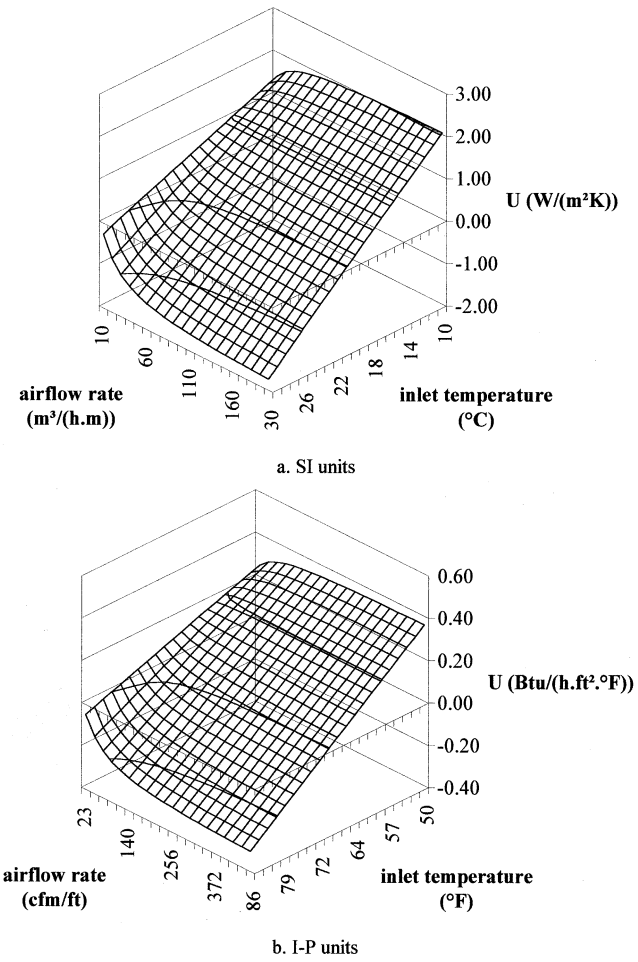

Figure 9 *U-factor of the mechanically ventilated active envelope with lowered shading device as a function of the inlet temperature and the airflow rate.*

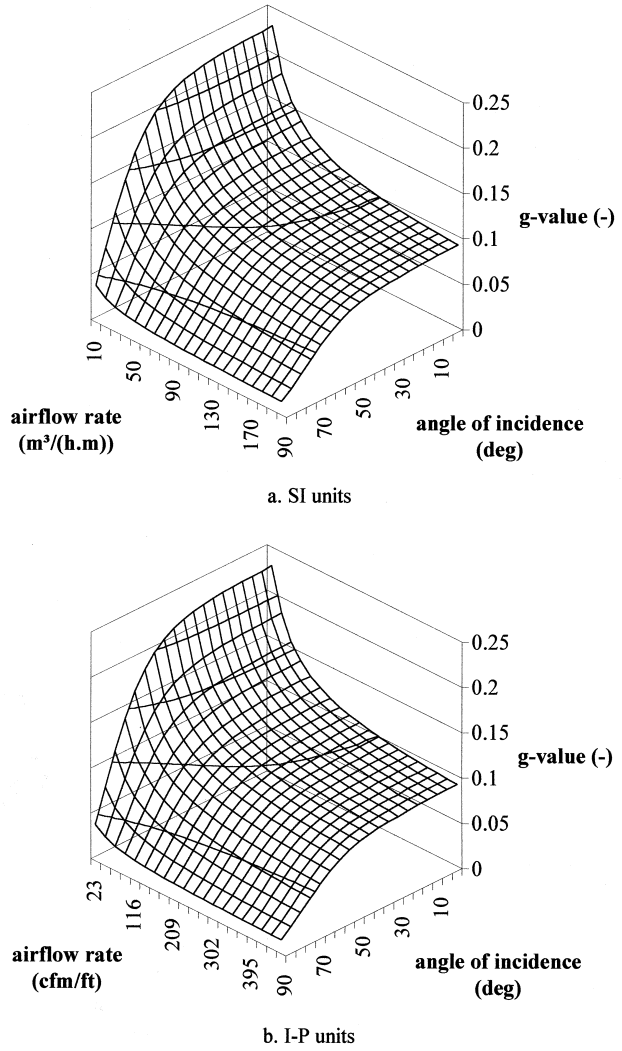

Figure 10 *G-value of the mechanically ventilated active envelope with lowered shading device as a function of the angle of incidence and the airflow rate.*

unclear. The overall energy performance should be analyzed on building level and under actual climatic conditions.

CONCLUSIONS

Active envelopes are regularly presented as being energy-efficient envelope solutions. In this paper, a numerical model to evaluate the thermal behavior of active envelopes has been presented and compared with in situ measurements. The agreement between the measurements and the simulations is good for the mechanical flow active envelope. The natural flow active envelope is much more difficult to model due to the fact that the airflow rate cannot be predicted accurately.

The numerical model has been implemented in an energy simulation program, and an annual energy simulation has been performed on a select number of active envelope typologies. The results were compared to those of a traditional cladding system. Compared to the traditional cladding solution, active envelopes proved to have lower transmission losses but higher transmission gains. These results cannot, however, be extrapolated to the office heating and cooling load.

The naturally ventilated envelope has a somewhat higher heating load but a slightly lower cooling load than the traditional envelope. However, some reservations have to be made because of the uncertainty about the airflow rate in the cavity. Regarding mechanically ventilated active envelopes, the lower transmission gains of the mechanically ventilated active envelopes are offset by the enthalpy change of the cavity return air for airflow rates that surpass the ventilation airflow rate. In summer, we have to conclude that free cooling is an important measure in preventing overheating rather than that active envelopes reduce the cooling load.

The energy demand analysis shows that the energy performance strongly depends on the way the return cavity air is used. In order to correctly evaluate the energy efficiency of active envelopes, it is imperative to take into account the enthalpy change of the cavity air.

ACKNOWLEDGMENTS

This research is funded by a research grant of the Flemish Institute for the Promotion of Industrial Scientific and Technological Research (IWT: Vlaams Instituut ter Bevordering en Promotie van het Wetenschappelijk-Technologisch Onderzoek in de Industrie). Their financial contribution is gratefully acknowledged.

REFERENCES

ASHRAE. 1997. *1997 ASHRAE handbook—Fundamentals*. Atlanta: American Society of Heating, Refrigerating and Air-Conditioning Engineers, Inc.

Baker P., D. Saelens, M. Grace, and T. Inoue. 2000. Advanced envelopes—Methodology, Evaluation and design tools, Final report IEA Annex 32 (IBEPA). Leuven, Belgium: Acco.

Busselen, B., and P. Mattelaer. 2000. *E*xperimentele evaluatie van actieve gevelsystemen (in Dutch), Master's thesis. Leuven, Belgium, KU Leuven.

Compagno, A. 1995. *Intelligent glass facades—Material, practice, design*. Basel: Verlag für Architektur.

Edwards, D.K. 1977. Solar absorption by each element in an absorber-coverglass array. *Solar Energy* 19: 401-402.

Gertis, K. 1999. Sind neuere Fassadenentwickelungen bauphysikalisch sinnvoll? Teil 2: Glas-Doppelfassaden (GDF), (in German). *Bauphysik* 21: 54-66.

Hendriks, L., and H. Hens. 2000. Building Envelopes in a holistic perspective—Methodology, Final report IEA Annex 32 (IBEPA). Leuven, Belgium: Acco.

Hottel, H.C. 1954. Radiant-heat transmission. In McAdams, W.H. (ed.), *Heat Transmission*. New York: McGraw-Hill.

Liddament, M.W. 1996. *A guide to energy efficient ventilation*. Warwick: Air Infiltration and Ventilation Centre.

Park, S.D., H.S. Suh, and S.H. Cho. 1989. The analysis of thermal performance in an airflow window system model. *Thermal Performance of the Exterior Envelopes of Buildings IV.* Atlanta: American Society of Heating, Refrigerating and Air-Conditioning Engineers, Inc., pp. 361-375.

Saelens, D., and H. Hens. 1998. DVV case study—An overview of measurements during summer conditions, *Report STB-B-98/A2*, IEA Annex 32 *IBEPA*.

Saelens, D., and H. Hens. 1999. Low-energy design and airflow windows, some considerations illustrated with a case study. *Proceedings of the 10th International Symposium for Building Physics*, pp. 327-336.

Saelens, D., and H. Hens. 2001a. Experimental evaluation of airflow in naturally ventilated active envelopes. Accepted for publication in *Journal of Thermal Insulation and Building Science*.

Saelens, D., and H. Hens. 2001b. Modeling of air and heat transport in active envelopes. Accepted for publication in *Proceedings of ICBEST 2001, International Conference on Building Envelope Systems and Technologies*.

Siegel, R., and J.R. Howell. 1992. *Thermal radiation heat transfer.* London: Taylor and Francis.

Ziller, C. 1999. Modellversuche und Berechnungen zur Optimierung der natürlichen Lüftung durch Doppelfassaden (in German). PhD dissertation, Aachen, Shaker Verlag.